# ESTIMATING $M_s$ FROM SHORT-PERIOD (< 10 SEC) RAYLEIGH WAVES

Jessie L. Bonner,[1] David G. Harkrider,[1] Mark Leidig,[1] Eugene Herrin,[2] Robert H. Shumway,[3]
Sara A. Russell,[1] Ileana Tibuleac,[1] and Delaine T. Reiter[1]

Weston Geophysical Corporation,[1] Southern Methodist University,[2] University of California, Davis[3]

Sponsored by Air Force Research Laboratory

Contract No. DTRA01-01-0080

## ABSTRACT

Surface wave magnitude ($M_s$) estimation for small events recorded at near-regional distances will often require a magnitude scale designed for Rayleigh waves with periods less than 10 seconds. During the past year, we have examined the performance of applying two previously published $M_s$ scales on 7-second Rayleigh waves recorded at regional distances. First, we modified the Marshall and Basham (1972) $M_s$ scale, originally defined for periods greater than 10 seconds, which was developed to estimate surface wave magnitudes for short-period Rayleigh waves from earthquakes and explosions on or near the Nevada Test Site (NTS). We refer to this modification as $M_s$ [M+B;7], and we have used short-period, high-quality dispersion curves to determine empirical path corrections for the 7-second Rayleigh waves at the stations MNV, LAC, ELK, and KNB. We have also examined the performance of the Rezapour and Pearce (1998) formula, developed using theoretical distance corrections and surface wave observations with periods greater than 10 seconds, for 7-second Rayleigh waves, $M_s$ [R+P;7], recorded from the same dataset. The results demonstrate that both formulas can be used to estimate $M_s$ for nuclear explosions and earthquakes over a wider magnitude distribution than is possible using conventional techniques developed for 20 second Rayleigh waves. These $M_s(7)$ values scale consistently with other $M_s$ studies at regional and teleseismic distances with the variance described by a constant offset; however, the offset for the $M_s$ [M+B;7] estimates is over one magnitude unit closer to the teleseismic values than the $M_s$ [R+P;7] values. Using our technique, it is possible to employ a near-regional single-station or sparse network to estimate surface wave magnitudes, thus allowing quantification of the size of both small earthquakes and explosions. Finally, we used a jackknife technique to determine the false alarm rates for the $M_s$ [M+B;7]-$m_b$ discriminant for this region, and found that the probability of misclassifying an earthquake as an explosion is 10% while the probability of classifying an explosion as an earthquake was determined to be 1.2%. The misclassification probabilities are slightly higher for the $M_s$ [R+P;7] estimates.

We recently initiated a study aimed at examining the transportability of short-period $M_s$ to the Lop Nor test site. We developed averaged dispersion curves from large ($m_b$>5.5) nuclear tests at Lop Nor to generate path corrections for the stations AAK, BRVK, KUR, MAK, and TLY. We then estimated short-period $M_s$ for nuclear explosions and earthquakes at Lop Nor and determined that transportability of the $M_s$[M+B;7] -$m_b$ discriminant is more complicated due to deeper earthquakes at Lop Nor than at NTS. However, by using the period of maximum amplitude, instead of restricting ourselves to 7-seconds, and by calibrating path corrections to periods less than 10 seconds, we were able to improve the separation between the earthquake and explosion populations at Lop Nor using non-conventional estimates.

## OBJECTIVE

One of the most robust methods for discriminating between explosions and earthquakes is the relative difference between the body wave ($m_b$) and surface wave ($M_s$) magnitude for a seismic event. For a given $m_b$, earthquakes often generate substantially more surface wave energy than explosions and thus are characterized by a larger surface wave magnitude. Our research is aimed at determining if magnitudes obtained from surface waves recorded at near-regional distances and periods less than 10 seconds can be used to accurately characterize the size of a seismic source. The answer to this question is essential in determining our ability to discriminate lower yield events in the $3.5 < m_b < 4.5$ range. Levshin and Ritzwoller (2001) suggest this problem is difficult to answer because structural variations, which can alter short-period surface wave amplitudes by as much as 50%, have scales that cannot be resolved with current 3-D models, thus rendering path corrections difficult to determine. Also, short-period surface waves are more sensitive to high-frequency asymmetries in the shot cavity and spall. The fact remains, however, that at regional distances, surface wave trains are not well dispersed and explosions are often characterized by a pulse-like shape with dominant periods ranging from 5 to 12 seconds. Thus, it is difficult, and for small events often impossible, to determine an $M_s$ as it was originally defined for 20-second Rayleigh waves. Either a path-corrected, spectral magnitude (e.g. Stevens and McLaughlin, 2001; Stevens and Murphy, 2001) or an $M_s$ scale that can incorporate these shorter periods is required to examine the performance of the $M_s$-$m_b$ discriminant for small events recorded at regional distances. The objective of this research is to present the results of applying two established and popular $M_s$ formulas to regional Rayleigh-wave data with periods less than 10 seconds.

## RESEARCH ACCOMPLISHED

### Phase I: The Nevada Test Site

**Data.** We have estimated 7-second surface wave magnitudes for NTS explosions that occurred between December 1968 and September 1992. The primary research focus was on the 198 NTS explosions that were detonated after August 1979, for which digital data are available from the Lawrence Livermore Network (LNN) stations. Sixty-one (61) of these events have no LNN data available, are plagued by data dropouts and glitches, or are too small for measurable surface wave energy. We also analyzed 21 events prior to July 1979 that were digitized from analog records in order to compare these results with previous $M_s$ studies for NTS events completed by Yacoub (1983), Marshall *et al*., (1979), and Stevens and Murphy (2001). Thus, this paper presents the results of our analyses of 158 NTS explosions including 51 events from Pahute Mesa, 13 from Rainier Mesa, and 94 explosions from the Yucca Flats. We have also tabulated the location of the events relative to the water table and the lithology in which the event was detonated.

We also estimated the $M_s$ and $m_b$ magnitudes for 40 earthquakes whose locations are shown in Figure 1. The earthquake data consisted of LNN seismograms for events tabulated in Patton (2001; Table A.1) that were within 2 degrees of the NTS. This allowed us to maintain similar azimuthal coverage and propagation paths for the NTS explosions in our dataset. The Patton (2001) earthquake database has no events beyond 1994, thus we also downloaded data recorded at station NV31 for events between January 1999 and June 2002. This earthquake dataset, while not as extensive as our explosion database, has $m_b(Pn)$ (Patton, 2001) values ranging from 2.98 to 5.84 and depths ranging from 0 to 17 km.

**$m_b$ Estimation.** For our examination of the $M_s$-$m_b$ discriminant performance for small events in the Western United States (WUS), we required both regional $m_b$ and $M_s$ magnitude scales. Fortunately, an $m_b$ scale has already been developed and tested for the WUS. The Denny *et al.* (1987; 1989) body wave magnitude formula (referred to henceforth as the DTV $m_b$) was specifically developed for the WUS using an extensive database of earthquakes and nuclear explosions at or near the Nevada Test Site. Thus, all $m_b$s presented in this study are $m_b(Pn)$s estimated using the DTV equation and station constants. For most of the NTS explosions, we used the DTV $m_b$ determined by Vergino and Mensing (1989), and we used the DTV $m_b$ determined by Patton (2001) for most of the WUS earthquakes. For events in which no $m_b(Pn)$ was published, we used the DTV equation to calculate an average network $m_b(Pn)$ using the available LNN stations.

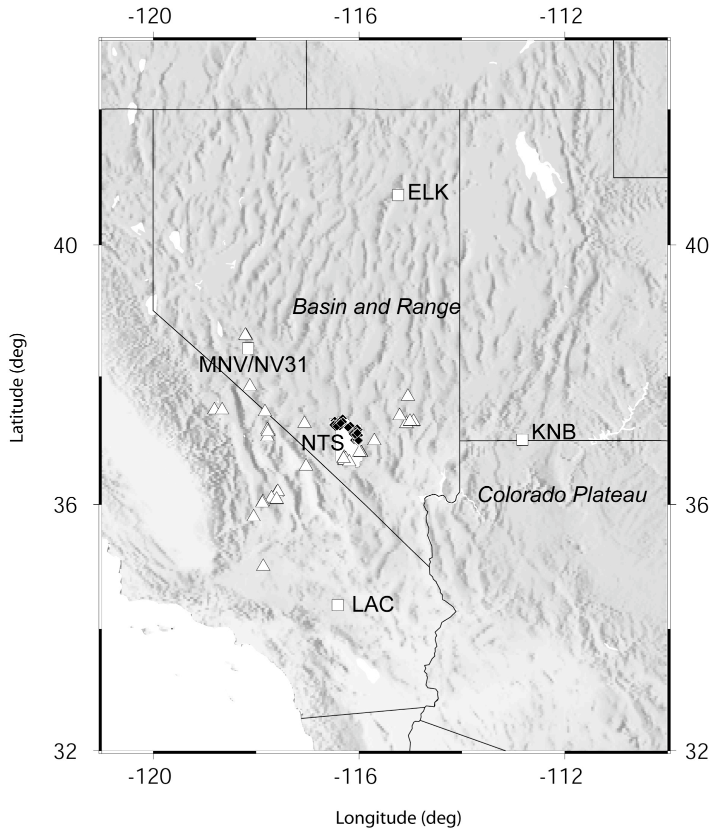


**Figure 1. The locations of the four LNN stations (squared), as well as earthquakes (triangles) and explosions (diamonds on the NTS) used in this study.**

***$M_s$*(7) from Marshall and Basham (1972).** Marshall and Basham (1972) reformulated the Prague formula (Vanek *et al.,* 1962) as:

$$M_s = \log_{10}(A) + B'(□) + P(T) \tag{1}$$

where A is the Rayleigh wave amplitude (zero-to-peak in nm), B'(□) is an attenuation correction as a function of distance (□) in degrees, and P(T) is a path correction as a function of period T. There is an additional term of 0.008*h*, where *h* is the depth of the event that can be included in Equation 1. Because depth is often difficult to determine for near-regional events, we did not apply a depth correction to the explosion and earthquake data in order to examine the discriminant performance assuming a surface focus. The distance corrections B'(□) used for this study are proportional to 0.8 $\log_{10}$ (□), as Basham (1971) showed this relation to be valid for earthquakes and explosions with an 8-14 second period at regional distances.

The path corrections listed in Table 2 of Marshall and Basham (1972) are not applicable to periods less than 10 seconds. The path correction P(T) is estimated from the amplitude of a group velocity (U) dispersion curve predicted by the method of stationary phase (Ewing *et al.*, 1957) with the expression

$$\frac{U}{T^{3/2}\sqrt{\frac{dU}{dT}}}\,.$$

The P(T) corrections are normalized to a 20-second period in order to compare the short-period results with conventional $M_s$ measurements. To generate the P(T) corrections, we used multiple filter analyses to generate group velocity dispersion curves for paths from NTS to MNV, ELK, KNB, and LAC. We averaged the dispersion curves for 8 NTS explosions with large Rayleigh-wave SNR ($m_b > 5.2$) between 5 and 20 seconds. We based our decision to make our surface wave measurements at a period of 7 seconds on two observations. First, a period of 7 seconds represents an average of the dominant periods for surface waves recorded at near-regional distances in the WUS.

Additionally, dispersion curves for paths in this region shows there is an inverse Airy phase (or a group velocity maximum) observable on the dispersion curves near approximately 9 seconds period, and it is best to retreat from the complications associated with this phenomenon when making amplitude measurements. As determined from the above expression, the P(T) corrections will become infinite at each Airy phase. We determined the P(7) corrections for each path, and the results are listed in Table 1. The P(7) corrections for paths to MNV, ELK, and LAC are essentially the same since these paths are all located within the Basin and Range tectonic province (Figure 1). The different dispersion curve for the path from NTS to KNB is caused by the thickening of the crust near the station associated with the transition from the Basin and Range to the Colorado Plateau (Keller *et al.*, 1976). We refer to our surface wave estimates for 7-second Rayleigh waves using Equation 1 and empirically calibrated path corrections as $M_s$ [M+B;7].

**Table 1. P(7) corrections for LNN Stations**

| Station | P(7) |
|---|---|
| MNV/NV31 | -0.79 |
| ELK | -0.79 |
| KNB | -0.56 |
| LAC | -0.73 |

***$M_s$*(7) from Rezapour and Pearce (1998).** Using the entire dataset from the International Seismic Center, Rezapour and Pearce (1998) developed a distance independent $M_s$ defined as:

$$M_s = \log\frac{A}{T} + \frac{1}{3}\log_{10}(\Delta) + \frac{1}{2}\log_{10}\left(\sin(\Delta)\right) + 0.0046\Delta + 2.370 \qquad (2)$$

where A is the zero to peak amplitude in nm, T is the period in seconds, and $\Delta$ is the distance in degrees. Unlike the Marshall and Basham (1972) formula that used empirical distance and path corrections (Equation 1), the Rezapour and Pearce (1998) equation was developed using theoretical aspects of dispersion and geometrical spreading. The formula was adopted by the prototype International Data Center in 1998 for calculating surface wave magnitudes at distances between 20 and 100 degrees; however, it is now used by the International Data Center to determine an $M_s$ for all surface waves recorded at distances less than 100 degrees (Stevens and McLaughlin, 2001). We note that the original Rezapour and Pearce (1998) paper presents no application of their formula at periods less than 10 seconds and at distances less than 20 degrees. For this study, we applied Equation 2 to short-period, near-regional data to determine $M_s$ [R+P;7] estimates for the same dataset as used for the modified Marshall and Basham (1972) formula.

**NTS Explosions.** We measured the amplitude for 7-second period Rayleigh waves for 158 NTS events recorded at MNV, ELK, KNB, and LAC and estimated both $M_s$ [M+B;7] and [R+P;7] for each event. We present a comparison of the network-averaged 7-second $M_s$ for all measured NTS events versus the DTV network $m_b(Pn)$ in Figure 2. Pahute Mesa, Rainier Mesa, and Yucca Flats events were analyzed and are presented as circles, stars, and triangles, respectively. We also denote the location of the water table, relative to each event, as either a solid symbol (events that were detonated above the water table) or an open symbol (events detonated below the water table). We regressed the [M+B;7] and [R+P;7] versus the DTV $m_b(Pn)$, and the resulting equations and standard deviations for each NTS test area are shown. The primary goals of our research are to present the applicability of the $M_s$(7) scale, and to highlight the fact that using the short-period data allows us to estimate surface wave magnitudes for 45 explosions with $m_b < 4.5$, as compared to one in the original Marshall and Basham (1972) paper, two in the Rezapour and Pearce (1998) paper, and less than ten in Stevens and McLaughlin (2001). In addition, we have determined $M_s$(7) measurements for 9 events with $3.7 < m_b < 4.0$.

**Comparison of the Near-Regional *$M_s$*(7) and Teleseismic *$M_s$*.** Of course, estimating near-regional $M_s$(7) values for NTS events that can be calibrated to conventional $M_s$ scales is of primary importance to our research as well. We compared our $M_s$ [M+B;7] and $M_s$ [R+P;7] estimates taken directly from the near-regional surface waves with the $M_s$ measurements obtained from a modeling technique derived by Woods and Harkrider (1995). Their indirect method of estimating $M_s$ consisted of modeling the surface waves recorded at regional distances, and then propagating the regional synthetics to distances of 40 degrees. At 40 degrees, the synthetics showed significant 20 second surface wave energy; thus Woods and Harkrider (1995) measured $M_s$ from the synthetics. Figure 3 shows the comparison of our $M_s$ [M+B;7] and $M_s$ [R+P;7] with $\pm 1\sigma$ plotted as the horizontal lines and the Woods and Harkrider (1995) indirect method (W+H) with $\pm 1\sigma$ plotted as vertical lines. We performed a fixed-slope (slope=1) linear regression to compare the $M_s(7)$ values with the Woods and Harkrider (1995) values and found a strong correlation. The offset shows that the $M_s$ [M+B;7] and $M_s$ [R+P;7] estimates are 0.20 m.u. lower and 0.95 m.u. higher, respectively, than the Woods and Harkrider (1995) estimates. Woods and Harkrider (1995) showed their measurements also correlated very well with conventional NTS $M_s$ values from Marshall and Basham (1972), Marshall *et al*. (1979), and Yacoub (1983) with considerable variance in the offsets. We also compared the performance of $M_s$ [M+B;7] and $M_s$ [R+P;7] with Yacoub (1983). The results for the comparison with Yacoub (1983) are shown also in Figure 3 and indicate similar scaling relationships based on the fixed-slope regression analysis. In this case, our $M_s$ [M+B;7] and $M_s$ [R+P;7] values are offset from Yacoub's (1983) estimates by approximately +0.02 m.u. and +1.21 m.u., respectively. Differences in these absolute estimates result from the use of different $M_s$ definitions, especially in the attenuation factors; however, these comparisons do show that our estimates are scaling similarly to other measurements of NTS surface wave magnitudes.

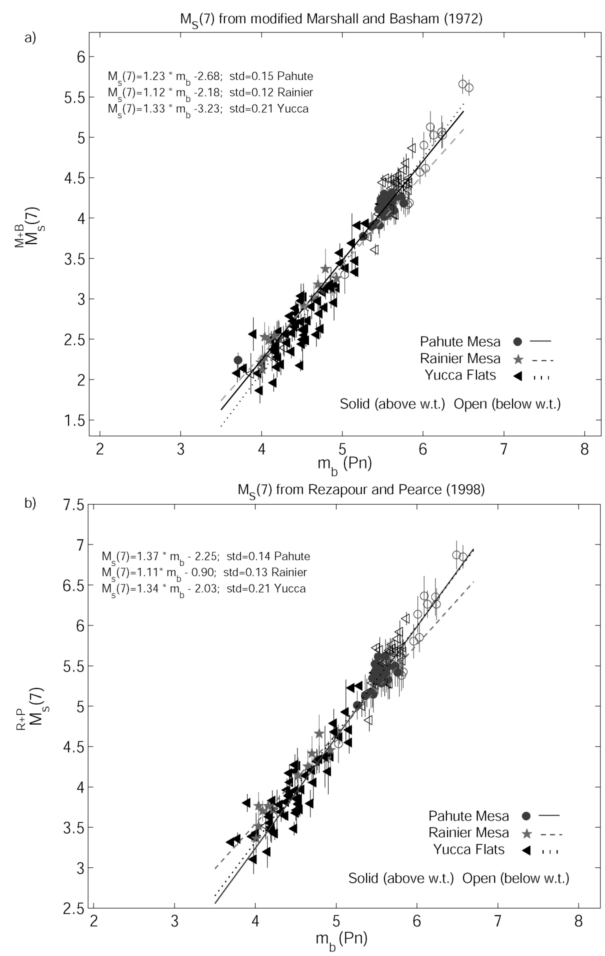


**Figure 2. Network-averaged 7-second $M_s$ estimates for 158 NTS events at Pahute Mesa, Rainier Mesa, and Yucca Flats regressed against $m_b(Pn)$. The best-fitting regression lines are plotted as solid (Pahute), dashed (Rainier), and dotted (Yucca) lines. Solid symbols indicate events above the water table (w.t.) with open symbols showing events below the water table. The vertical lines represent one standard deviation for the $M_s$ estimate.**

The properties of Rayleigh wave propagation make it difficult to develop a single expression that gives consistent $M_s$ values at both regional and teleseismic distances. Figure 4 presents the comparison of near-regional $M_s$ estimates (i.e. $M_s$ [M+B;7] and $M_s$ [R+P;7]) with far-regional and teleseismic estimates of $M_s$ using the same formulas (i.e. Marshall and Basham (1972) and Rezapour and Pearce (1998) formulas, respectively). Marshall *et al.* (1979) used the Marshall and Basham (1972) $M_s$ formula for far-regional and teleseismic distance recordings of NTS events for Rayleigh waves with periods greater than 14 seconds. We determined that the near-regional $M_s$ [M+B;7] estimates have a similar scaling relationship when using a fixed slope (slope = 1.00) regression analysis, but are consistently

0.35 m.u. higher than Marshall *et al*. (1979) for the 5 events in their dataset for which we had LNN data to analyze. We note that most of our near-regional estimates have better azimuthal coverage than Marshall *et al.* (1979) who mainly used Canadian data and thus may have strong azimuthal biases. This could be a possible source for the consistent difference. Another source could be the attenuation terms; however, we do not have data at a wide enough distance range in this study to verify the appropriateness of Basham (1971) as the correct attenuation model.

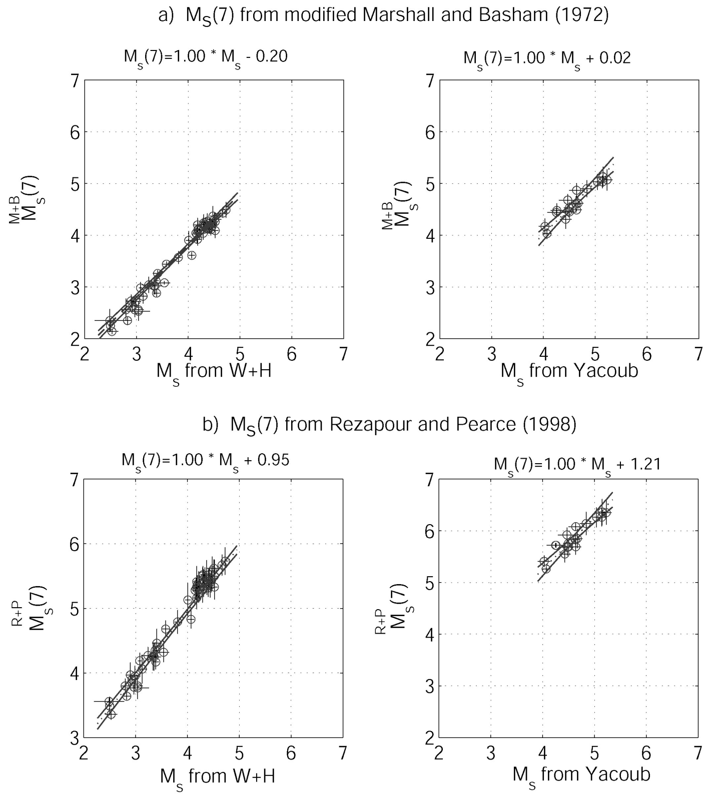


**Figure 3. A comparison of our 7-second $M_s$ estimates for NTS with the Woods and Harkrider (1995) indirect estimates (W+H; left) and Yacoub (1983; right). The best-fitting regression line, with a fixed slope = 1.0, is given by the dotted line running through the data points, and it is surrounded by the pointwise 95% confidence intervals plotted as two solid lines.**

We observed that the $M_s$[R+P;7] estimates are on average 1.6 m.u. larger than the Marshall *et al.* (1979) teleseismic $M_s$ values.

The Rezapour and Pearce (1998) formula has not been tested significantly at near-regional distances and short periods until this paper, and our results suggest there are considerable differences between the short-period, near-regional magnitudes and teleseismic magnitude estimates for NTS events. We regressed our $M_s$ [R+P;7] estimates versus far-regional and teleseismic $M_s$ estimates (Figure 4) determined by Stevens and Murphy (2001) using the Rezapour and Pearce (1998) formula. We note consistent scaling between the two estimates, however, there is an offset of +1.46 m.u. We note much better agreement between the Stevens and Murphy (2001) teleseismic $M_s$ values and the 7-second modified Marshall and Basham (1972) estimates. Thus, we believe path corrections will be required for correct application of the Rezapour and Pearce (1998) formula at near-regional distances and periods less than 10 seconds.

**Earthquakes and Discriminant Analysis.** We measured the amplitude for 7-second period Rayleigh waves for 40 earthquakes (Figure 1) within 2 degrees of the NTS as recorded at MNV (or the collocated NV31), ELK, KNB, and LAC and estimated a $M_s$ [M+B;7] and $M_s$ [R+P;7] for each event. We then examined the performance of the modified Marshall and Basham (1972) and Rezapour and Pearce (1998) $M_s$(7)-$m_b$ discriminants for earthquakes and explosions. The populations of earthquakes and explosions suggest that $M_s$ and $m_b$ will be fitted well by linear regressions, with approximately equal slopes assumed for the earthquake and explosion populations. Although we did observe slightly different slopes in the regression analyses for the two populations, we believe that this is due to inadequate sampling of earthquakes at $m_b$ magnitudes greater than 4.5. Our dataset does not present any evidence that the two populations are converging at smaller magnitudes, although other $M_s$-$m_b$ studies (Stevens and McLaughlin, 2001) suggest that convergence does occur. Furthermore, it seems sensible to regard the $M_s$ values as dependent variables, observed conditionally on fixed values for $m_b$, which are more accurately determined in the WUS when the DTV $m_b$ (Denny *et al.*, 1987; 1989) formula is applied. This yields the following regression model:

$$M_s = \alpha_i + \beta m_b + e \tag{3}$$

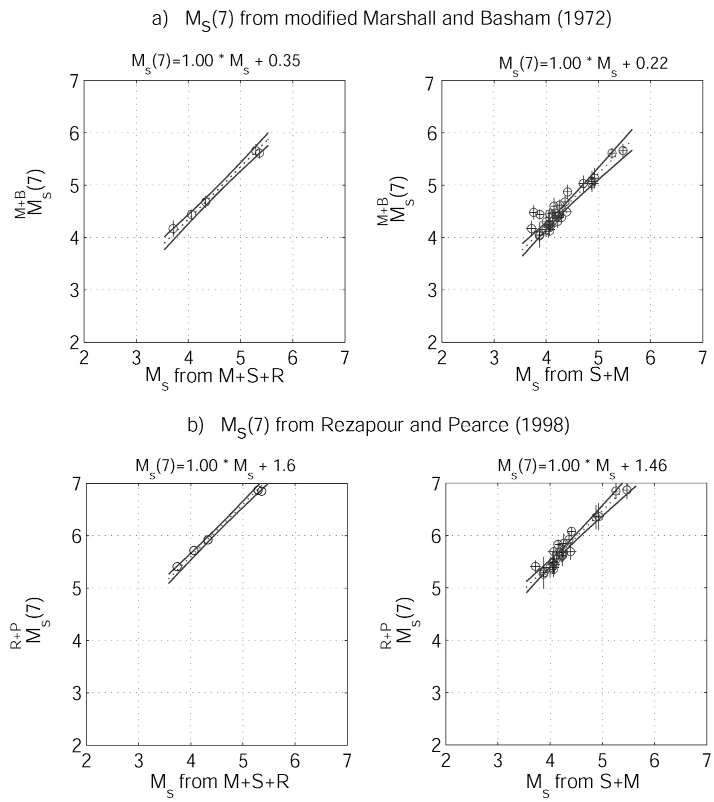


**Figure 4. A comparison of our 7-second $M_s$ estimates for NTS with the Marshall *et al.* (1979) estimates (M+S+R; left) and Stevens and Murphy (2001) estimates (S+M; right).**

i=1,2 where the intercepts $\alpha_1$ and $\alpha_2$ correspond to the earthquake (Q) and explosion (X) populations respectively. Under this approach, the errors (e) are assumed to be independent and identically distributed normal variables. For determining the optimal discriminant functions, the parallel regression assumption with independent normal errors seems more sensible than the usual assumption of bivariate normality used to get the classification function. Hence, we proceed to use the linear function following from the conditional regression approach to discrimination. This leads to a discriminant function of the form:

$$d = M_s - \frac{1}{2}(\alpha_1 + \alpha_2) - \beta m_b. \tag{4}$$

With equal prior probabilities, we classify an event of unknown origin as an earthquake if d>0 and as an explosion otherwise. The classification criterion in the equal slope case is then applied with the values estimated from the data. We note first the result of applying the discriminant function, d, directly, as shown in Figure 5. Note the four misclassified earthquakes in the $M_s$[M+B;7]-$m_b$ plot and the six misclassified earthquakes in the $M_s$[R+P;7]-$m_b$ case. To estimate the performance of the discriminant function (Equation 4), we used a jackknifing technique where the observation to be classified is held out during the estimation of the slope and intercept procedure and then the discriminant function is applied to the observation to be classified using the estimated parameters. For the $M_s$[M+B;7] case, we misclassified 4 earthquakes as explosions (10%) while only classifying two explosions (1.2%)

as earthquakes. The misclassification rates are slightly higher for the $M_s$[R+P;7] estimates as we identified 6 earthquakes (16%) as explosions and 3 explosions (2%) as earthquakes.

**<u>Phase II: The Lop Nor Test Site Preliminary Results</u>**

Our next stage of the research project was to examine the applicability of short-period $M_s$ scales on the Lop Nor Test site in western China. We followed the same procedures as outlined above and generated path corrections for Equation 1. We averaged the group velocity dispersion curves of four large Lop Nor nuclear explosions recorded at AAK, BRVK, MAK, KUR, and TLY and the results are shown in Figure 6. We then estimated the path corrections for these dispersion curves, and the results are also provided in Figure 6 in addition to the dashed line, which shows

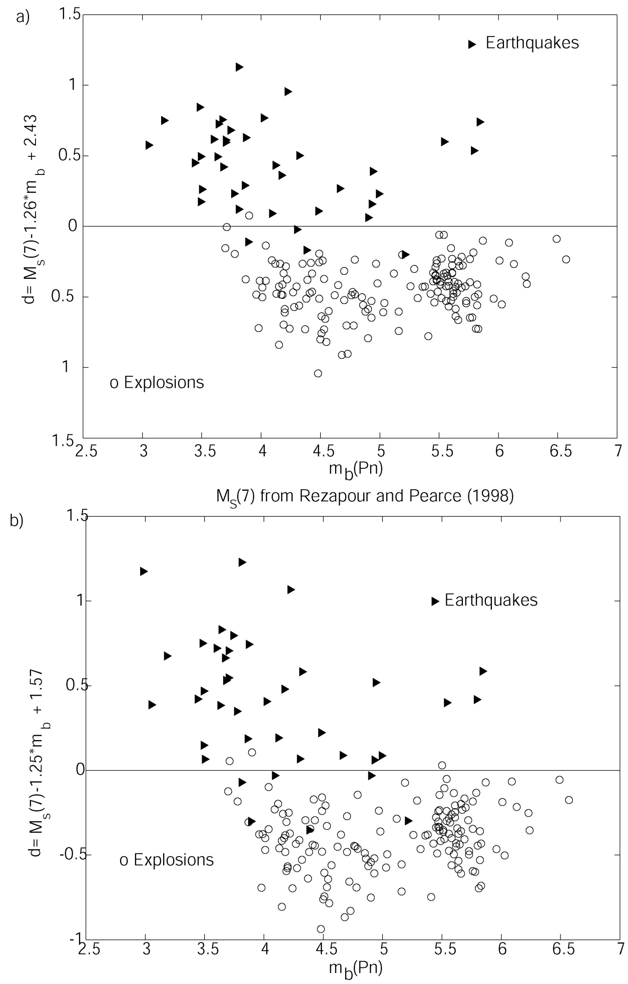


**Figure 5. Discriminant functions for a) $M_s$[M+B;7] and b) $M_s$[R+P;7] for earthquakes and explosions considered in this study. The parameter □ from Equation 4 represents the slope (1.26 and 1.25) of the $m_b$ versus $M_s$ populations and the decision line is determined from the means for both populations. Based upon our evaluation of the $M_s$[M+B;7] -$m_b$ relationship for this region, we calculated the probability of misclassifying an earthquake as an explosion as 10% and the probability of classifying an explosion as an earthquake to be 1.2%. The results are slightly worse for $M_s$[R+P;7] -$m_b$ , where 15% of the earthquakes are misclassified as to be explosions and 2% of the explosions labeled as earthquakes.**

the path corrections for Marshall and Basham's (1972) "Eurasia". The variability in the dispersion curves and resulting path corrections highlight the need for improved regional calibration, which is being completed in China by Maceira and Taylor (2003). We then used these path corrections to determine $M_s$[M+B;7] for six explosions and for five earthquakes located on or near the Lop Nor test site. The results of plotting them versus USGS $m_b$ are shown in Figure 7 and highlight the problems associated with restricting our analysis to 7-second Rayleigh waves.

While this formed a robust discriminant for events near NTS, we see that there is inadequate offset in the two populations for our current small dataset. Two of five earthquakes could not be statistically distinguished from the explosions. We believe the poor performance is related to the effect of source depth on 7-second Rayleigh wave generation. All five of these earthquakes have reported depths greater than 14 km resulting in reduced 7-second surface wave generation.

To improve the discrimination analysis, we returned to the original definition of the Marshall and Basham (1972) formula which stated that the period used to calculate $M_s$ should be where the maximum amplitude in the surface wave train occurs. For these five explosions recorded at regional distances, the maximum amplitude occurred at periods between 8 and 10 seconds. Thus, we used the path corrections for the period of maximum amplitude and calculated $M_s$ [M+B; Max], and unlike Marshall and Basham (1971), we did not limit ourselves to periods greater than 10 seconds. We recalculated the earthquake magnitudes in the same manner; however, the period of maximum amplitude ranged from 8 to 18 seconds. The results are also shown Figure 7, and in this case there is increased separation among the populations. We note that the recent (13 March 2003) event located near the Lop Nor test site falls within the earthquake population for both methods. We plan to add more earthquake and explosion data to this analysis within the next year to better understand short-period surface wave estimation at Lop Nor and elsewhere.

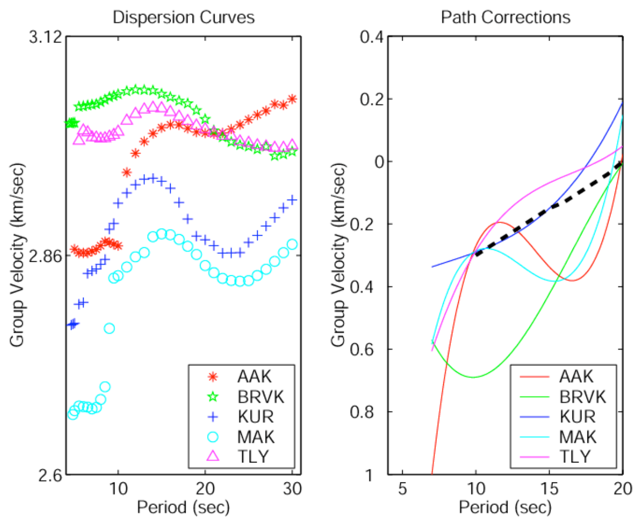


**Figure 6. Left) Dispersion curves for paths from Lop Nor to regional stations. Right) Path corrections as a function of period.**

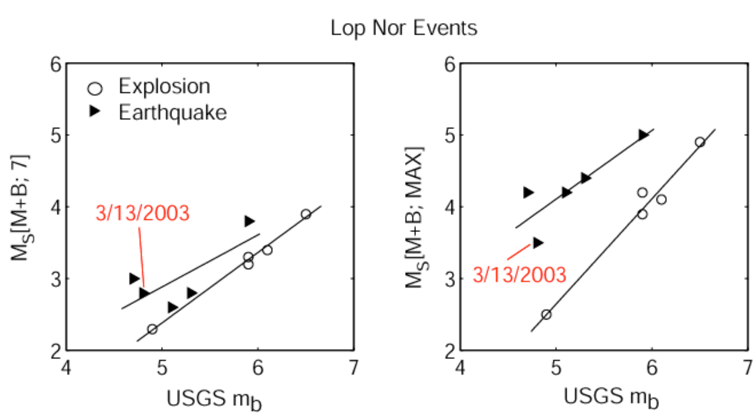


**Figure 7. An examination of network averaged surface wave measurements for events on or near Lop Nor calculated with (left) 7-second Rayleigh waves and (right) the period (between 8 and 18 seconds) of the maximum Rayleigh wave amplitude.**

## CONCLUSIONS AND RECOMMENDATIONS

The $M_s$[M+B;7] -$m_b$ and $M_s$[R+P;7] -$m_b$ discriminants defined in this paper can now be used as tools to help screen explosions from earthquakes in the vicinity of the Nevada Test Site (NTS). The false classification rates for the method are small, and the method can be used in conjunction with other regional NTS discriminants, such as the phase and spectral ratios (Walter *et al*., 1995) and body wave and moment magnitude ratios ($m_b$-$M_w$) (Patton, 2001). Transportability of the $M_s$[M+B;7] -$m_b$ discriminant to Lop Nor was complicated due to deeper events than at NTS. However, by using the period of maximum amplitude instead of 7-second only and by calibrating path corrections to periods less than 10 seconds, we were able to increase the separation between the earthquake and explosion populations at Lop Nor. There is important information related to source size and depth in short-period surface waves, and our work will continue to improve the regional path corrections required to improve the accuracy in magnitude estimation.

## ACKNOWLEDGMENTS

We are indebted to Howard Patton for his assistance in database acquisition and his comments concerning various aspects of the research. We also wish to thank Bill Walter for help in acquiring the MNV dataset. We express our gratitude to Marv Denny, Jeff Stevens, Nazeih Yacoub, Steve Taylor, Nancy Cunningham, Shelly Johnson, and James Lewkowicz for insightful discussions about the manuscript and research.

## REFERENCES

Basham, P.W. (1971), A new magnitude formula for short-period continental Rayleigh waves, *Geophys. J. R. Ast. Soc.,* **23**, 255.

Denny, M.D., S. R. Taylor, and E.S. Vergino (1987), Investigation of $m_b$ and $M_s$ formulas for the western United States and their impact on the $M_s/m_b$ discriminant, *Bull. Seism. Soc. Am.,* **77**, 987-995.

Denny, M.D., S. R. Taylor, and E.S. Vergino (1989), Erratum: Investigation of $m_b$ and $M_s$ formulas for the western United States and their impact on the $M_s/m_b$ discriminant, *Bull. Seism. Soc. Am.,* **79**, 230.

Ewing, W.M., F. Press, and W.S. Jardetzky (1957), *Elastic waves in layered media,* McGraw-Hill, New York.
Herrmann, R. B. (2002). Computer Programs in Seismology Version 3.15, St. Louis University.

Keller, G.R., R.B. Smith, L.W. Braile, R. Heaney, and D.H. Shurbet (1976), Upper crustal structure of the eastern Basin and Range, northern Colorado plateau, and middle Rocky Mountains from Rayleigh-wave dispersion, *Bull. Seism. Soc. Am.,* **67**, 869-876.

Levshin, A.L. and M.H. Ritzwoller (2001), Automated detection, extraction, and measurement of regional surface waves, *Pure Appl Geophys*, **158**, 1531 - 1545.

Maceira, M. and S. R. Taylor (2003), Short-period surface wave tomography in central Asia and its application to seismic discrimination, *Seism. Res. Letts*., 74, p 212.

Marshall, P.D. and P.W. Basham (1972), Discrimination between earthquakes and underground explosions employing an improved $M_s$ scale, *Geophys. J. R. Astr. Soc*., **29**, 431-458.

Marshall, P.D., Springer, D.L, and Rodean, H.C. (1979), Magnitude corrections for attenuation in the upper mantle, *Geophys. J. R. Astr. Soc.,* **57**, 609-638.

Patton, H. (2001), Regional magnitude scaling, transportability, and $M_s$-$m_b$ discrimination at small magnitudes, in *Monitoring the Comprehensive Nuclear Test Ban Treaty: Source Processes and Explosion Yield Determination*, eds. Ekstrom, G., M. Denny, and J.R. Murphy, *Pure Appl. Geophys*., **158**, 1951-2015.

Rezapour, M., and R.G. Pearce (1998), Bias in surface-wave magnitude $M_s$ due to inadequate distance correction, *Bull. Seism. Soc. Am.,* **88**, 43-61.

Stevens, J.L., D.A. Adams, and E. Baker (2001), Surface wave detection and measurement using a one-degree global dispersion grid, *SAIC Final Report SAIC-01/1085*.

Stevens, J. L. and K.L. McLaughlin (2001), Optimization of surface wave identification and measurement, in *Monitoring the Comprehensive Nuclear Test Ban Treaty: Surface Waves*, eds. Levshin, A. and M.H. Ritzwoller, *Pure Appl. Geophys*., **158**, 1547-1582.

Stevens, J. L. and J.R. Murphy (2001),Yield Estimation from Surface-wave Amplitudes, in *Monitoring the Comprehensive Nuclear Test Ban Treaty: Surface Waves*: *Source Processes and Explosion Yield Determination*, eds. Ekstrom, G., M. Denny, and J.R. Murphy, *Pure Appl. Geophys*., **158**, 2227-2251.

Vanek, J., A. Zatopek, V. Karnik, Y.V. Riznichenko, E.F. Saverensky, S.L. Solov'ev, and N.V. Shebalin (1962), Standardization of magnitude scales, *Bull. (Izvest.) Acad. Sci. U.S.S.R., Geophys. Ser.,* **2**, 108.

Vergino, E.S. and Mensing, R.W. (1989), Yield estimation using regional $m_b(Pn)$, *Lawrence Livermore National Laboratory Report UCID-101600*.

Walter, W. R., K.M. Mayeda, and H.J. Patton (1995), Phase and spectral ratio discrimination between NTS earthquakes and explosions. Part I. Empirical Observations. *Bull. Seism. Soc. Am*., **85**, 1050-1067.

Woods, B. and D.G. Harkrider (1995), Determining surface-wave magnitudes from regional Nevada Test Site data, *Geophys. J. Int.,* **120**, 474.

Yacoub, N.K. (1983), Instantaneous amplitudes: a new method to measure seismic magnitude, *Bull. Seism. Soc. Am.,* **73**, 1345-1355.